IMAGE FIDELITY: IMPLICATIONS FOR ALMA

M.C.H. Wright
Radio Astronomy Laboratory, University of California, Berkeley, CA 94720 E-mail:
mwright@astro.berkeley.edu

ABSTRACT

This memo presents the case for adding smaller antennas to the ALMA array. Smaller, higher precision antennas are better able to exploit the excellent submillimeter potential of the 5000 m altitude site, and are better matched to the angular size of many submillimeter sources. Model studies show that the image fidelity of mosaiced observations with the ALMA array will be limited by pointing and surface errors. This can be understood in terms of the errors in the spatial frequencies derived from the mosaicing process. Spatial frequencies derived from the outer parts of the antennas, which serve to knit together the mosaic, may have larger errors than estimated from the overall surface and pointing RMS values. Adding smaller, higher precision antennas is a unique contribution which a Japanese collaboration could make to improve the submillimeter performance of ALMA, and also the image fidelity of mosaiced millimeter observations.

1. Introduction

Many astronomical studies require a comparison of images with a wide range of spatial scales. At millimeter wavelengths all but the most compact sources require mosaiced observations in order to image a wide range of angular scales. For example, the planned ALMA array with 12 m antennas at a wavelength of λ 1.2 mm has a field of view of only $20''$; angular scales larger than this must be obtained from mosaic observations. This includes most planets, star formation regions, galaxies and clusters of galaxies. After the sensitivity limited experiments have been done, and as the instrument matures, quantitative comparisons of images obtained in different wavebands will become more common. The proportion of projects which use mosaic observations with the BIMA array has increased by about 10% per year for the last 5 years.

With the ALMA array we may expect that eventually most images will be mosaics. Mosaics with *thousands* of pointings requiring on-the-fly mosaicing may be common (Holdaway 1994, MMA memo 122). Cornwell, Holdaway & Uson (1993; hereafter CHU93) showed that mosaiced images with a homogeneous array sample all spatial frequencies between zero and the maximum interferometer baseline provided the data are properly sampled. The *image fidelity* — how closely the image represents the real source distribution — depends not only on random noise but also on errors in the data, sampling, and imaging artifacts. CHU93 show that an image fidelity of 20, measured as the on-source signal to noise ratio requires an RMS surface accuracy of $\lambda/40$

and an antenna pointing accuracy of about 6% of the primary beam FWHM. This has become the basis of the antenna specification for the ALMA telescope, currently configured as sixty four 12 m antennas, with the above specifications at a wavelength of λ 1 mm. With a 25 μm overall surface accuracy, and a 5000 m altitude, the ALMA telescope will be be able to observe at submilleter wavelengths, for example, to image 450 μm dust emission, or CO J=7-6 emission at 372 μm. However our ability to make quantitative comparisons between images of dust emission in different wavebands, or line ratios in different transitions, will be limited by the relatively poor image fidelity, especially at submillimeter wavelengths. This memo discusses the image errors from homogeneous and heterogeneous arrays

2. Image Errors

In mosaiced observations, pointing and surface errors introduce phase errors into the Fourier components which are derived from the phase gradients across the aperture at each pointing. In a single pointing observation, the antenna pointing and surface errors modify the illumination of the field of view, and are second order errors in the visibility data for objects which are small compared with the primary beam. Of course, beyond the FWHM of the primary beam pattern, large systematic errors may occur, and for objects which fill an appreciable fraction of the primary beamwidth, the image fidelity is poorer than for mosaiced observations. These effects are usually ignored and no primary beam correction is usually applied in presenting single pointing images.

CHU93 present model simulations which show the degradation of the image fidelity as a function of pointing and surface errors. These predictions are verified in practice. In a mosaic image of the supernova remnant Cas A at 83 GHz, using the BIMA array we obtained an image fidelity 1% to 2% of the peak intensity (Wright etal 1999). This image combined multifrequency synthesis at multiple configurations of the BIMA array to obtain adequate uv sampling. Data from 75 to 87 GHz were combined into a single MFS, mosaiced image with a mean frequency of 83 GHz (λ 3.6 mm). The BIMA antennas have an overall surface RMS of 30 micron; $\lambda/120$ at 83 GHz. The RMS pointing is 5″; 4% of the primary beam FWHM at 83 GHz. Analysis of the imaging errors shows that residual primary beam and pointing errors each contribute about 1% to the image errors.

Although the overall surface accuracy and pointing are more than adequate for 3 mm observations, in routine observing conditions, the focus and subreflector position are not at their optimum settings. The net result is that the illumination of the source is not exactly as described by the primary beam model used in the mosaiced image which consequently limits the image fidelity of the large scale structure. We found that the image fidelity was improved by spatial filtering. By excluding the low spatial frequencies which were derived from single dish observations and the mosaicing process, we measured structures smaller than 95″ to 1-2%, but were only able to measure larger scale structure to about 10% (on-source RMS/PEAK intensity).

The surface accuracy of the outer 30% to 50% of the antennas is critical. Consider for example

an antenna constructed of panels 1 square meter. The panel RMS is 7 μm. The overall antenna RMS is 30 μm. In practice, the deviation from a parabola of the inner parts of the antenna are better than 30 μm, and the outer parts are worse than 30 μm. Spatial frequencies which are determined by a small number of outer panels contain substantial errors which are correlated from panel to panel, due to gravitational and thermal deflections.

For example, if the typical deviation in the outer panels is 50 μm, and there are 9 independent measurements of a spatial frequency which is derived from the path difference between sections of the antenna surface on either the same or adjacent antennas, then the path error is 2 x sqrt(2) / sqrt(9) x 50 μm. This is 18 deg of phase at λ 1 mm, and 40 deg of phase at λ 450 μm. Although in principle a homogeneous array gives a reasonably flat response as a function of spatial frequency, the surface accuracy of the outer 30% to 50% of the antennas is critical. Welch (MMA memo 134, figure 1) shows the spatial response for the short spacings with proper accounting for the illumination taper. We expect that a similar situation will obtain for the ALMA antennas.

3. Heterogeneous Arrays

The Cas A observations led to a series of model studies to investigate the imaging performance of the combined California array, currently known as CARMA. The combined array will have six 10.4 m antennas and nine 6.1 m antennas and possibly a similar number of 2.5 - 3 m antennas designed for microwave background experiments. This heterogeneous array is well suited to a wide range of projects and is not optimized for single pointing, sensitivity limited observations. BIMA memo 73 presents an empirical study of the image fidelity obtained as a function of the *uv* sampling, the pointing sampling, and the image complexity. We imaged three representative models: multiple compact sources, Cas A, and eye charts. The Cas A model and the eye charts are extended, complex sources with a similar distribution of spatial scales from 0.5″ to a few arcmin, and give similar results. It is easier to appreciate the image defects on the eye charts. We compared the results obtained with homogeneous and heterogeneous arrays. A heterogeneous array allows shorter *uv* spacings to be sampled directly using a compact configuration of the smallest antennas. This reliably recovered more of the total flux density and the corresponding large scale structure. The heterogeneous CARMA array produced better image fidelity than a homogeneous array with the same number of antennas and collecting area. By historical accident, the CARMA array has about the right ratio of antenna sizes to produce good image fidelity for mosaics. Figure 1 shows an example of an eyechart image. Although the RMS is within 7% in both residual images the ratio of intensities of the eye chart letters has large errors. These results are discussed more fully in BIMA memo 73 (http://bima.astro.umd.edu/memo/memo.html).

Imaging with a heterogeneous array presents no fundamental problems. The existing imaging algorithms work with mixed antenna sizes, but may not be optimum. In a previous memo (MMA memo 180), we concluded that the additional complexity of imaging with heterogeneous arrays was a vote in favor of a homogeneous array. Fortunately, the software has improved considerably

over the last few years, so that the complexity is hidden from the user. Making a mosaiced image using the MIRIAD software looks the same to the user as single field imaging (Sault etal, 1996). The image is formed as a primary beam weighted linear mosaic for all primary beam types. The primary beam pattern for each antenna can be different. Deconvolution of a common model, consistent in a least squares sense with the data for each observation, is properly weighted by the primary beam patterns.

These developments provide a model for the future development of the ALMA array. Adding small, high precision antennas to the current ALMA array is a unique contribution which a Japanese collaboration could make to improve not only the submillimeter performance of ALMA, but also the image fidelity of mosaiced millimeter observations.

4. Observing Strategies

The smaller antennas are well suited for mapping large source structure, and are best placed at short baselines in order to sample uv spacings down to the diameter, D_{min} of the smallest antenna. Shorter uv spacings, between 0 and D_{min} can be obtained from single dish observations with the larger antennas. Since we depend less on the outer parts of the antenna surfaces than in the case of the homogeneous array, the fidelity of these spatial frequencies is improved.

For many projects it is desirable to have approximately the same single dish sensitivity as the interferometer data. This is important for detecting and mapping large angular size sources, especially transient sources such as comets. This argues for using several of the larger antennas for single dish observations. Using the larger antennas on the longest interferometer baselines provides a more uniform sensitivity in the uv data and reduces the required uv data sample rate.

A heterogeneous array provides an overlap in the spatial frequencies derived from direct interferometer observations with the smaller antennas, and from the single dish observations with the larger antennas. This overlap provides additional constraints on the calibration of these data.

4.1. Single dish observations

Independent of whether one has a heterogeneous or homogeneous array, we still need single dish observations to measure the lowest spatial frequencies. These typically contain the most power, and errors will seriously corrupt the images. Single dish observations measure spatial frequencies in a similar way to the mosaiced observations. As we scan the antenna across the source, the phase gradient across the wavefront is multiplied by the errors and illumination of the aperture surface. A single dish observation is a zero spacing mosaiced observation with the additional complication of atmospheric variations in the measured total power. It seems clear that the single dish data will ultimately limit the image fidelity of mosaiced images. Better data can be obtained with improved single dish observing techniques, such as sampling the data rapidly as

the subreflector and the antenna scan across the source. If the atmosphere is well behaved, then we should be able to deconvolve the motion of a frozen atmospheric screen across the source by repeated observations with a scanning subreflector.

5. Conclusions

At submillimeter wavelengths the performance of the ALMA array will probably be limited, not by sensitivity, but by uncorrected primary beam and pointing errors.

We submit that an image fidelity of 10 to 20 – a 10% to 5% RMS error in the measured brightness distribution – is not a very high standard for a $0.5 billion state-of-the-art telescope on a superb 5000 m altitude site.

This memo suggests that adding smaller antennas to the current homogeneous array of 12 m antennas will enhance both the sub-millimeter performance, and the imaging performance at millimeter wavelengths.

More attention needs to be given to improving single dish observing techniques which are an integral part of mosaicing observations.

REFERENCES

Cornwell, T.J., 1988, A&A 202, 316
Cornwell, T.J., Holdaway, M.A., & Uson, J.M. 1993, A&A 271, 697
Ekers, R. D., & Rots, A.H. 1979, in IAU Col. 49, *Image Formation from Coherence Functions in Astronomy* , ed. van Schooneveld, C. (Dordrecht:Reidel), p.61
Welch, Wm.J., 1995, MMA memo 134
Wright, M.C.H., 1991, BIMA memo 73
Wright, M., Dickel, J., Koralesky, B., & Rudnick, L., 1999, ApJ, 518, 284
Cornwell, T.J., 1989, Synthesis Imaging in Radio Astronomy. Ed. R.A. Perley, F.R. Schwab, & A.H.Bridle, ASP Conf. Ser. 6, 277
Holdaway, M.A., 1997, MMA Memo 177
Holdaway, M.A., 1994, MMA Memo 122
Sault, R.J., Staveley-Smith, L & Brouw, W.N., 1996, A&A Supp., 120, 375

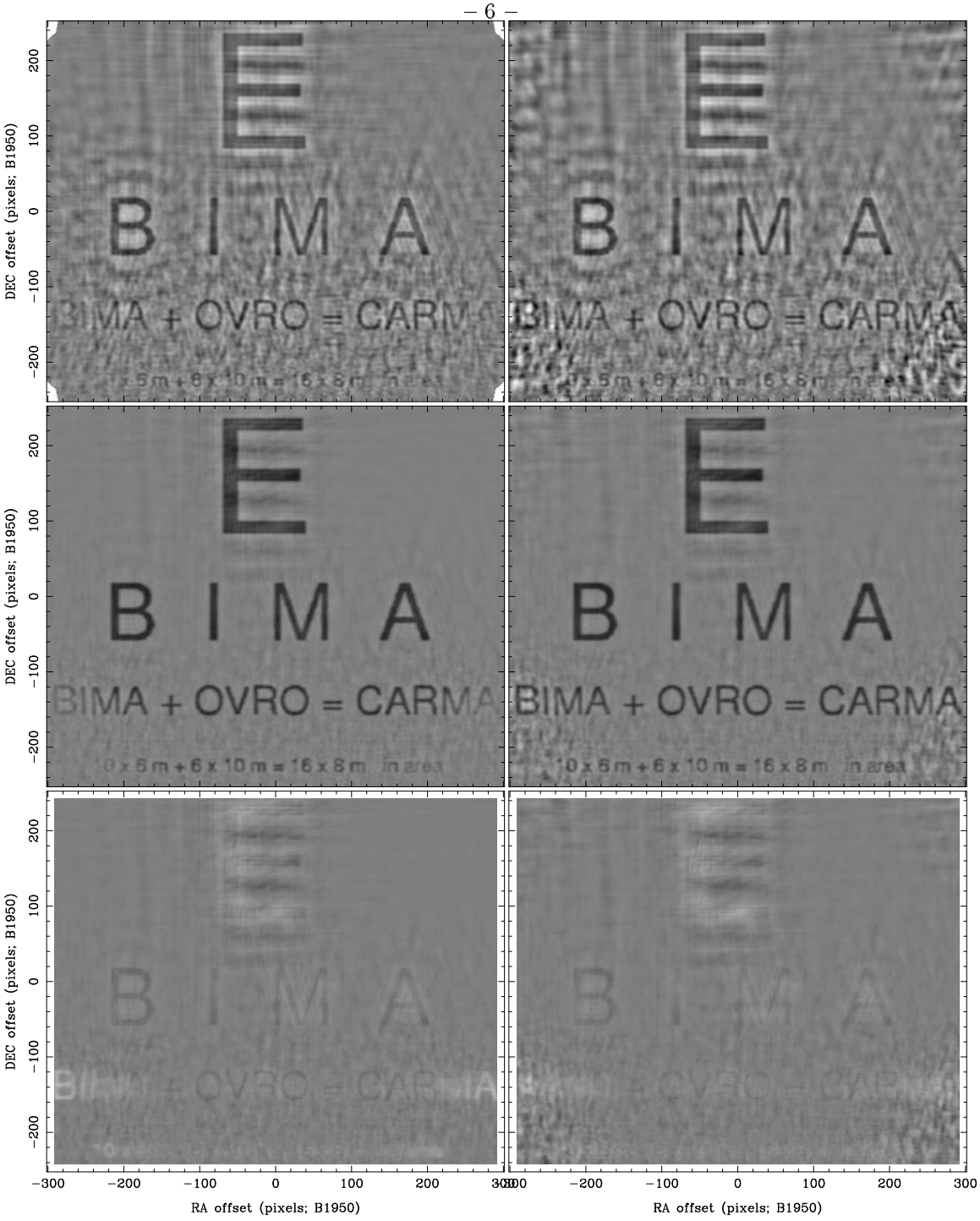

Fig. 1.— Comparison of homogeneous and heterogeneous arrays. Left column: Images made with 19 pointings of a homogeneous array consisting of fifteen 8 m antennas at 100 GHz. Right column: Images made with 19 pointings of the heterogeneous, CARMA array, consisting of six 10.4 m and nine 6.1 m antennas. Top: mosaiced images. Middle: Maximum Entropy deconvolution. Bottom: The RMS residual is within 7% in both mosaics; the heterogeneous mosaic has better image fidelity of the eye chart letters.